

Design of C_1 -symmetric tridentate ligands for enantioselective dearomative [3 + 2] annulation of indoles with aminocyclopropanes

Received: 14 September 2022

Accepted: 12 April 2023

Published online: 20 April 2023

Check for updates

Hai-Xia Wang^{1,3}, Chun Yang^{1,3}, Bai-Yu Xue¹, Ming-Sheng Xie¹✉, Yin Tian²✉, Cheng Peng² & Hai-Ming Guo¹✉

Chiral polycyclic indolines are widely present in natural products and have become the focus of extensive synthetic efforts. Here, we show the catalytic asymmetric dearomative [3 + 2] annulation of indoles with donor-acceptor aminocyclopropanes to construct tricyclic indolines. Key to the success of the reaction is the rational design of C_1 -symmetric bifunctional tridentate imidazoline-pyrroloimidazolone pyridine ligand. Under 5 mol% of $Ni(OTf)_2$ -ligand complex, diverse tricyclic indolines containing cyclopentamine moieties are obtained in good chemoselectivities, high diastereoselectivities, and excellent enantioselectivities. An unusual *cis*-configuration ligand is superior to the *trans*-configuration ligand and the corresponding C_2 -symmetric tridentate nitrogen ligands in the annulation reaction. Mechanistic studies by control experiments and density functional theory calculations reveal a dual activation manner, where $Ni(II)$ complex activates the aminocyclopropane via coordination with the geminal diester, and imidazolidine NH forms a H-bond with the succinimide moiety.

Chiral polycyclic indolines exist widely in natural products, which often contain cyclic amine fragments, such as vindolinine¹, *N*-methylkopsanone², and vincadifformine³ (Fig. 1a). For their construction, catalytic asymmetric dearomatization (CADA) reaction of indoles is a powerful strategy^{4–11}. In 2013, Tang and co-workers pioneered the highly enantioselective cyclopentannulation of indoles with donor-acceptor (D-A) aryl cyclopropanes catalyzed by a chiral side armed bisoxazoline (SaBox)- $Cu(OTf)_2$ complex^{12–17}. Later, Waser and co-workers reported the catalyzed reaction of D-A aminocyclopropanes with C3-substituted indoles, producing C2-

alkylated products instead of [3 + 2] annulation products (Fig. 1b)¹⁸. In 2019, Wang and co-workers developed Rh(II) carbene triggered cyclopentannulation reaction to form diverse polycyclic indolines with high yields, in which D-A aminocyclopropanes were formed in situ (Fig. 1c)¹⁹. In 2021, Waser and co-workers described the catalytic [3 + 2] annulation of D-A aminocyclopropane monoesters and indoles in high yields and diastereoselectivities catalyzed by triethylsilyl triflimide²⁰. In order to construct chiral tricyclic indolines containing cyclopentamine moieties, we envisaged the utilization of the catalytic asymmetric dearomative [3 + 2] annulation reaction of

¹State Key Laboratory of Antiviral Drugs, Pingyuan Laboratory, Key Laboratory of Green Chemical Media and Reactions, Ministry of Education, Collaborative Innovation Center of Henan Province for Green Manufacturing of Fine Chemicals, School of Chemistry and Chemical Engineering, Henan Normal University, Xinxiang, Henan 453007, China. ²State Key Laboratory of Southwestern Chinese Medicine Resources, School of Pharmacy, Chengdu University of Traditional Chinese Medicine, Chengdu 611137, China. ³These authors contributed equally: Hai-Xia Wang, Chun Yang. ✉e-mail: xiemingsheng@htu.edu.cn; ytian227@outlook.com; [ghm@htu.edu.cn](mailto:g hm@htu.edu.cn)

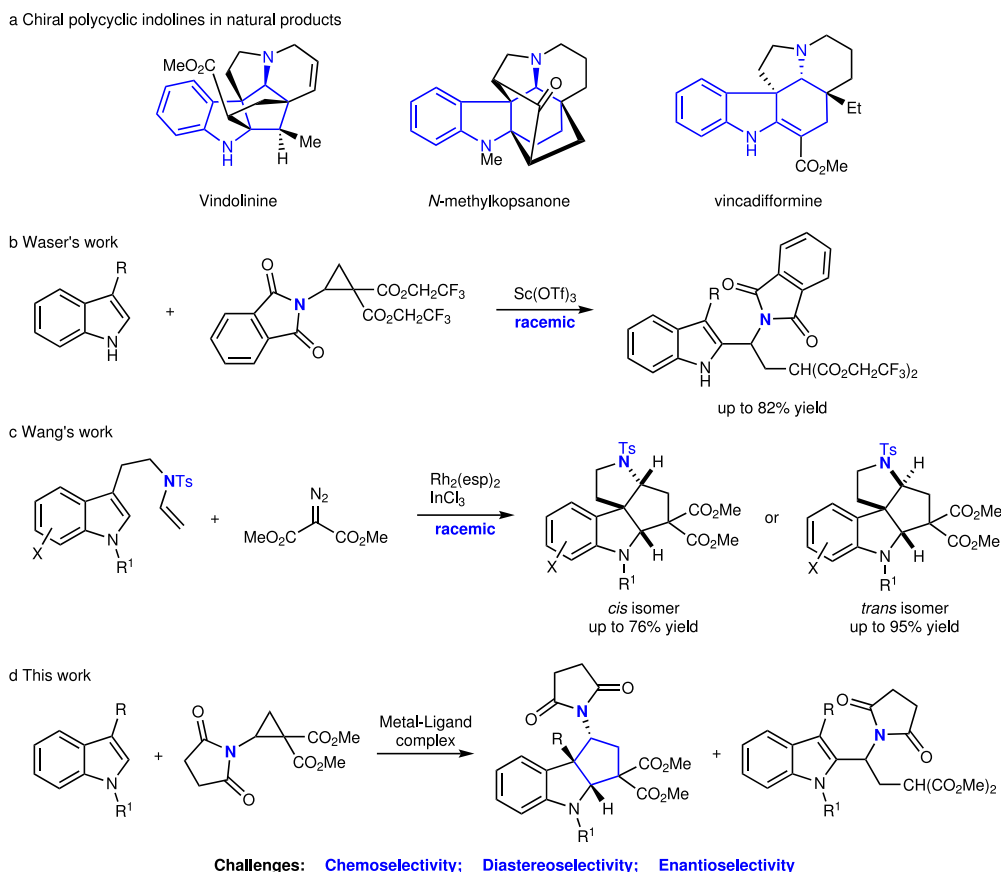


Fig. 1 | Significances and reactions of D-A cyclopropanes with substituted

indoles. **a** Chiral polycyclic indolines containing cyclic amine fragments in natural products. **b** Previous work: the reaction of D-A aminocyclopropanes with C3-substituted indoles produces C2-alkylated product from Waser et al. **c** Previous

work: Rh(II) carbene triggered cyclopropanation reaction of in situ formed D-A aminoacyclopropanes from Wang et al. **d** This work: catalytic asymmetric dearomative [3 + 2] annulation reaction of D-A aminocyclopropanes with C3-substituted indoles. D-A donor–acceptor.

D-A aminocyclopropanes with C3-substituted indoles. However, this approach possesses some challenges related to chemo-, diastereo-, and enantioselectivity (Fig. 1d).

The design and development efficient chiral tridentate nitrogen ligands bearing a pyridine ring is an attractive goal in asymmetric catalysis^{21–28}. C_1 -Symmetric tridentate nitrogen ligands have the ability to connect two different chiral moieties, hence, exhibit a greater capacity for structural tuning. Notable C_1 -symmetric tridentate nitrogen ligands include pyridyl-based benzimidazolyl-oxazolyl ligand²⁹, bis(imino)pyridine³⁰, iminopyridine-oxazoline (IPO)^{31,32}, oxazoline aminoisopropylpyridine (OAP), imidazoline iminopyridine (IIP) and thiazoline iminopyridine (TIP)³³. In 2010, Arai and co-workers developed bis(imidazolidine)pyridine (PyBidine) as a highly efficient bifunctional tridentate nitrogen ligand with imidazolidine NH as H-bond donor, and proved that imidazolidine was a privileged chiral moiety^{34,35}. Recently, in 2022, our group reported bis(pyrroloimidazolone)pyridine (PyBPI) as a bifunctional tridentate ligand, in which pyrroloimidazolone framework^{36,37} formed a non-flat chiral fence³⁸. By incorporating imidazoine and pyrroloimidazolone into the pyridine skeleton, we designed a C_1 -symmetric tridentate imidazoline-pyrroloimidazolone pyridine (PyIPI) ligands (Fig. 2a).

PyIPI ligand was readily synthesized from pyridine-2,6-dicarbaldehyde in twice condensation reactions with L-prolinamide and (*R,R*)-diphenylethylenediamine, respectively. PyIPI ligand readily formed a metal complex with Cu(OTf)₂, which was determined by X-ray diffraction analysis of a single crystal (Fig. 2b). The central Cu metal displayed a pentacoordinated square pyramidal geometry, where three nitrogen atoms and two triflate ligands were bonded to

the central metal. Furthermore, H-bonding existed between the imidazolidine NH atom and one oxygen atom of triflate anion, with a distance of 2.439 Å. We hypothesized that PyIPI may exhibit the following features: (1) the tridentate nitrogen ligand could coordinate with different Lewis acids, and imidazolidine NH could act as H-bond donor, thus playing a bifunctional role; (2) the bicyclic pyrroloimidazolone moiety formed a non-flat chiral fence, and exerted an enhanced steric hindrance effect; (3) the configuration of newly formed sp³ carbons was tunable, resulting in greater catalyst variability; (4) the steric hindrance of two amine moieties could remotely control the chiral environment created by a tridentate nitrogen ligand; (5) the two different chiral sources were cheap and readily available.

In this work, we envisage that PyIPI coordinates with a metal to activate the aminocyclopropane via bidentate coordination with two carbonyl oxygen atoms, and imidazolidine NH forms a H-bond with the oxygen atom in succinimide moiety, thus resulting in a dual activation and creating a good stereocontrol in [3 + 2] annulation with indoles (Fig. 2c).

Results

Optimization study

Initially, the reaction of indole **1a** with racemic succinimido-substituted dimethyl ester cyclopropane **2a** was selected as the model reaction under PyIPI **L1** as the chiral ligand in CH₂Cl₂ at 25 °C (Table 1). When Cu(OTf)₂ was used as the central metal salt, the reaction proceeded in low yield, affording a mixture of tricyclic indoline **3a** and C2 alkylation product **4a** in a ratio of 83:17, in which

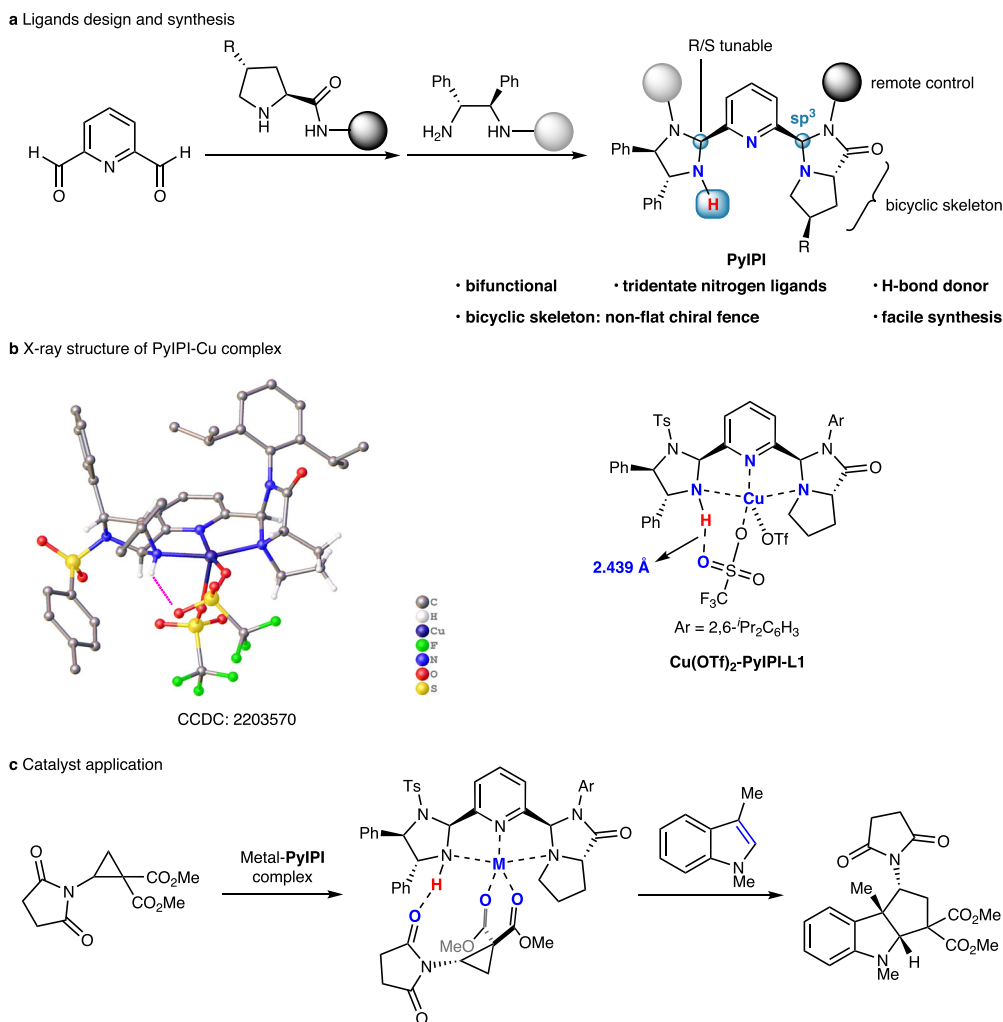


Fig. 2 | Design, synthesis, and application of PyIPI ligands. **a** Design and synthesis of PyIPI ligands. **b** X-ray structure of $\text{Cu}(\text{OTf})_2$ -PyIPI **L1** complex. **c** Metal-PyIPI complex catalyzed asymmetric dearomative [3 + 2] annulation of

indoles with donor–acceptor aminocyclopropane. PyIPI imidazoline-pyrroloimidazolone pyridine.

major product **3a** had 7:1 diastereoselectivity and 81% ee (entry 1). Hence, several metal salts were evaluated (entries 2–8), where $\text{Ni}(\text{OTf})_2$ showed the best results (91% total yield, **3a/4a** = 80:20, 8:1 dr, and 83% ee, entry 7). In the case of PyIPI **L2**, derived from *trans*-4-hydroxyl-L-prolinamide, low ee of **3a** was observed (entry 9). Chiral PyIPI **L3–L6** that contained different sterically hindered amide substituents were tested (entries 10–13). PyIPI **L4**, bearing a phenyl group on aniline, exhibited higher catalytic activity and enhanced stereocontrol (entry 11). Hence, PyIPI **L4** was used as the ligand to examine different nickel salts such as $\text{Ni}(\text{BF}_4)_2 \cdot 6\text{H}_2\text{O}$, $\text{Ni}(\text{ClO}_4)_2 \cdot 6\text{H}_2\text{O}$, and $\text{Ni}(\text{OAc})_2$. However, the obtained results did not show any enhancement (Supplementary Table 1). (*S,S*)-Diphenylethylenediamine derived PyIPI **L7** with a common *trans*-configuration was employed, resulting in a dramatic decrease in ee value of product **3a** (entry 14), indicating the importance of the unusual *cis*-configuration in **L4**. Utilization of C_2 -symmetric tridentate nitrogen ligands **L8** and **L9** showed low catalytic activity and poor ee values (entries 15 and 16), which illustrated the significance of C_1 -symmetry in **L4**. Increasing the ratio of aminocyclopropane **2a** to 2.2 equiv., further improved ee value of **3a** with 98% ee (entry 17). Altering the catalytic loading demonstrated that 5 mol% of $\text{Ni}(\text{OTf})_2$ -**L4** complex was optimal; however, even 2.5 mol% of catalyst still afforded product **3a** in 95% ee (entries 18 and 19). In comparison, other commonly used chiral ligands, such as chiral

bisoxazoline (Box) and pyridine-bisoxazoline (Pybox) were also tested. However, with ^tBu-Box or ^tBu-Pybox as ligands and $\text{Ni}(\text{OTf})_2$ as the central metal, the reaction did not happen under the same conditions (entries 20 and 21).

Scope of the reaction

Under optimal reaction conditions (Table 1, entry 18), the substrate scope of the asymmetric dearomative [3 + 2] annulation was explored (Fig. 3). Compared with 5-methyl- and 5-methoxy-substituted indoles **1b** and **1c**, the reaction of 5-chloro- and 5-bromo-substituted indoles **1d** and **1e** were slower, while the influence of electronic effect on enantioselectivity was negligible (**3b–3e**). 6-Bromo-substituted indole **1f** afforded annulation product **3f** in satisfactory results. C3-Allyl-substituted indole **1g** and C3-alkoxy-substituted indoles **1h–i** also proceeded smoothly, delivering tricyclic indoline **3g–i** in good results with 93–97% ee. In the case of penta-fused indole **1j**, [3,3,3,0]-tetracyclic indoline **3j** was obtained in 96% ee, albeit with low diastereoselectivity. Meanwhile, the reaction of 1,2,3-trimethylindole **1k** also proceeded well, delivering indoline **3k** in 65% yield, 4:1 dr, and 97% ee. It should be pointed out that indoles without a C3 substituent usually afforded only the products of Friedel-Crafts at C3 position, rather than the expected [3 + 2] annulation products (Supplementary Fig. 5). *N*-Benzyl indole **1l** gave [3 + 2] annulation product **3l** in good results. With 3-phenylindole **1m** as the reactant, the [3 + 2] annulation reaction could be occurred

Table 1 | Optimization of the reaction conditions^a

Reaction scheme: 1a + (±)-2a $\xrightarrow[\text{CH}_2\text{Cl}_2, \text{N}_2, 25^\circ\text{C}]{\text{Metal-PyPPI (x mol\%)}}$ 3a + 4a

Ligand definitions:
 L1: R = H; Ar = 2,6-*i*-Pr₂C₆H₃
 L2: R = OH; Ar = 2,6-*i*-Pr₂C₆H₃
 L3: R = H; Ar = 2,6-Et₂C₆H₃
 L5: R = H; Ar = 1-naphthyl
 L6: R = H; Ar = Bn

Entry	Metal	L	x	Yield ^b (%)	3a/4a ^c	dr ^c	ee ^d (%)
1	Cu(OTf) ₂	L1	10	23	83:17	7:1	81
2	Sc(OTf) ₃	L1	10	82	68:32	5:1	2
3	Yb(OTf) ₃	L1	10	Trace			
4	Mg(OTf) ₂	L1	10	0			
5	Fe(OTf) ₃	L1	10	75	70:30	7:1	53
6	Co(OTf) ₂	L1	10	79	79:21	8:1	69
7	Ni(OTf) ₂	L1	10	91	80:20	8:1	83
8	Zn(OTf) ₂	L1	10	65	80:20	8:1	73
9	Ni(OTf) ₂	L2	10	95	78:22	6:1	36
10	Ni(OTf) ₂	L3	10	93	80:20	9:1	89
11	Ni(OTf) ₂	L4	10	95	82:18	10:1	95
12	Ni(OTf) ₂	L5	10	92	81:19	10:1	92
13	Ni(OTf) ₂	L6	10	95	77:23	10:1	92
14	Ni(OTf) ₂	L7	10	90	76:24	6:1	-11
15	Ni(OTf) ₂	L8	10	38	75:25	8:1	15
16	Ni(OTf) ₂	L9	10	25	80:20	9:1	-2
17 ^e	Ni(OTf) ₂	L4	10	98	82:18	10:1	98
18 ^e	Ni(OTf) ₂	L4	5	98	82:18	10:1	98
19 ^e	Ni(OTf) ₂	L4	2.5	74	80:20	10:1	95
20	Ni(OTf) ₂	^t Bu-Box	5	0			
21	Ni(OTf) ₂	^t Bu-Pybox	5	0			

^aReaction conditions: Metal/L (1:1.2, x mol%), **1a** (0.1 mmol), **2a** (0.2 mmol) in CH₂Cl₂ (2.0 mL) at 25 °C under N₂ for 24 h.

^bThe total yield (**3a** + **4a**) was determined by ¹H NMR spectra of the crude product.

^cThe ratio of **3a/4a** and dr value of **3a** was determined by ¹H NMR spectra of the crude product.

^dThe ee value of **3a** was determined by chiral HPLC analysis.

^e**2a** (0.22 mmol).

with Cu(OTf)₂-**L4** as the catalyst, affording the tricyclic product **3m** in 51% yield, 1.8:1 dr, and 95% ee. Maleimido-substituted dimethyl ester cyclopropane **2b** was successfully reacted, affording annulation adduct **3n** in good results. Replacing the succinimide group with phthalimide increased reactivity but decreased enantioselectivity (**3a** vs **3o**). With thymine-substituted D-A aminocyclopropane **2d** as the reactant, the [3 + 2] annulation could proceed under Cu(OTf)₂-**L4** as the catalyst, affording chiral thymine carbocyclic nucleoside analog **3p** in 81% yield, 1.9:1 dr, and 67% ee. The absolute configuration of **3a** was

assigned by X-ray diffraction analysis. The relative configuration of diastereomer **3o'** was also assigned by X-ray crystallography.

Kinetic resolution experiment and scale-up reaction

In the above [3 + 2] annulation reaction, excess aminocyclopropane (2.2 equiv.) was used, which influenced ee value of **3a**. Thus, the kinetic resolution of aminocyclopropane **2a** was performed (Fig. 4a). At 62% conversion, recovered aminocyclopropane **2a** was obtained in 87% ee, and product **3a** was obtained in 40% yield, 8:1 dr, and 95%

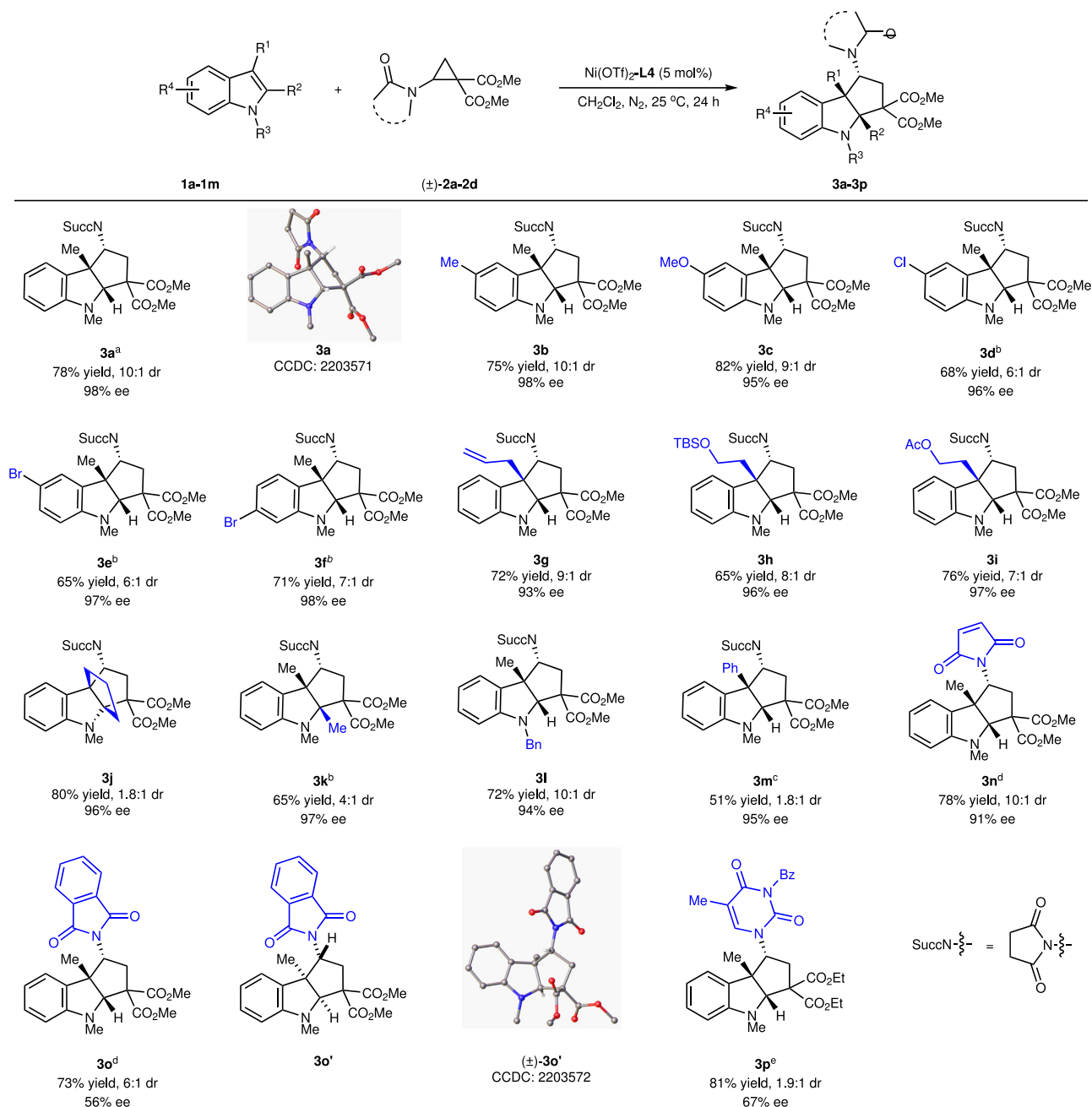


Fig. 3 | Substrate scope of the reaction. Unless otherwise noted, reaction conditions are as follows: Ni(OTf)₂/L4 (1:1.2, 5 mol%), **1** (0.2 mmol), **2** (0.44 mmol) in CH₂Cl₂ (4.0 mL) at 25 °C under N₂ for 24 h. Isolated total yields for product **3** (both diastereoisomers) were reported. The dr value was determined by ¹H NMR spectra of the crude product. The ee value was determined by chiral HPLC analysis.

a Reaction conditions: **1a** (0.3 mmol), **2a** (0.66 mmol) in CH₂Cl₂ (6.0 mL).
b Reaction time: 36 h. **c** Reaction conditions: Cu(OTf)₂/L4 (1:1.2, 10 mol%) at 50 °C for 64 h. **d** Reaction temperature: 0 °C. **e** Reaction conditions: Cu(OTf)₂/L4 (1:1.2, 10 mol%) at 35 °C.

ee. Furthermore, a gram-scale synthesis of tricyclic indoline **3a** was carried out (Fig. 4b). Using 5 mol% of Ni(OTf)₂-PyIPI **L4**, 4 mmol of indole **1a** reacted smoothly with aminocyclopropane **2a**, affording 1.12 g (70% yield) of product **3a** with 11:1 dr and 96% ee. After recrystallization, indoline **3a** was obtained as a pure enantiomer (63% yield, 99% ee).

Mechanistic studies

To understand the mechanism of the reaction catalyzed by Ni(OTf)₂-PyIPI **L4**, a series of control experiments were performed (Fig. 5). Firstly, ligand **L10**, the *N*-Me derivative of **L4**, was evaluated, generating product **3a** in low yield (45%) and reduced enantioselectivity (67% ee). This indicated that N–H proton on the imidazolidine moiety was

crucial for enhanced reactivity and enantioselectivity. In the case of ligand **L11**, bearing a phenyl ring instead of pyridine ring, only trace amount of product **3a** was obtained. By eliminating the pyrroloimidazolone moiety (ligand **L12**), once again only trace amount of product **3a** was obtained. When ligands **L13** and **L14**, lacking imidazolidine moieties, were examined, the yields and enantioselectivities were poor. Therefore, according to the obtained data the tridentate nitrogen coordinated to Ni(II) ion was essential for reactivity and stereocontrol.

Examination of the relationship between the enantioselectivity of ligand **L4** and product **3a** (Fig. 6) revealed a linear correlation in the catalytic reaction, which indicated that the species, 1:1 ratio of **L4** to Ni(II), may be the active catalytic species for the reaction.

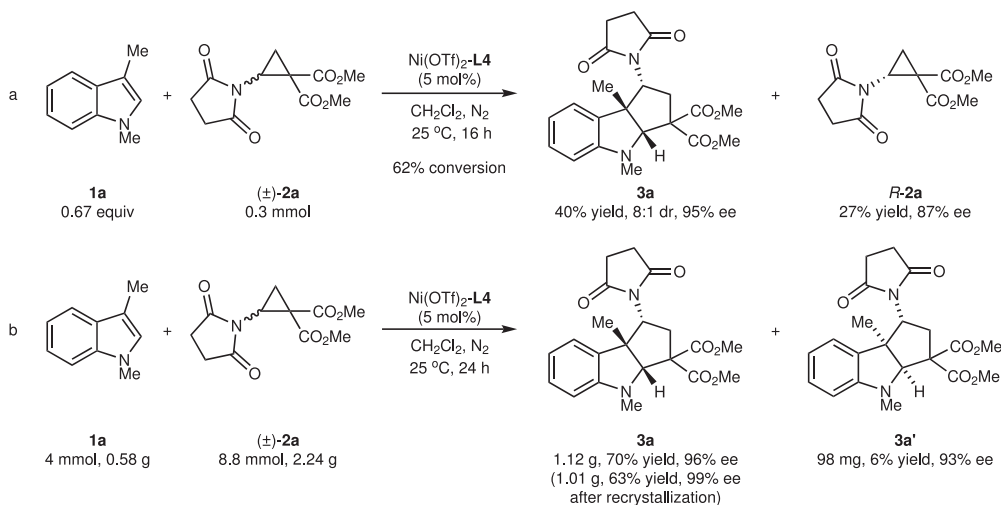


Fig. 4 | Kinetic resolution experiment and scale-up reaction. a Kinetic resolution experiment of 3-methylindole **1a** with aminocyclopropane **2a**. **b** Gram-scale synthesis of tricyclic indoline **3a**.

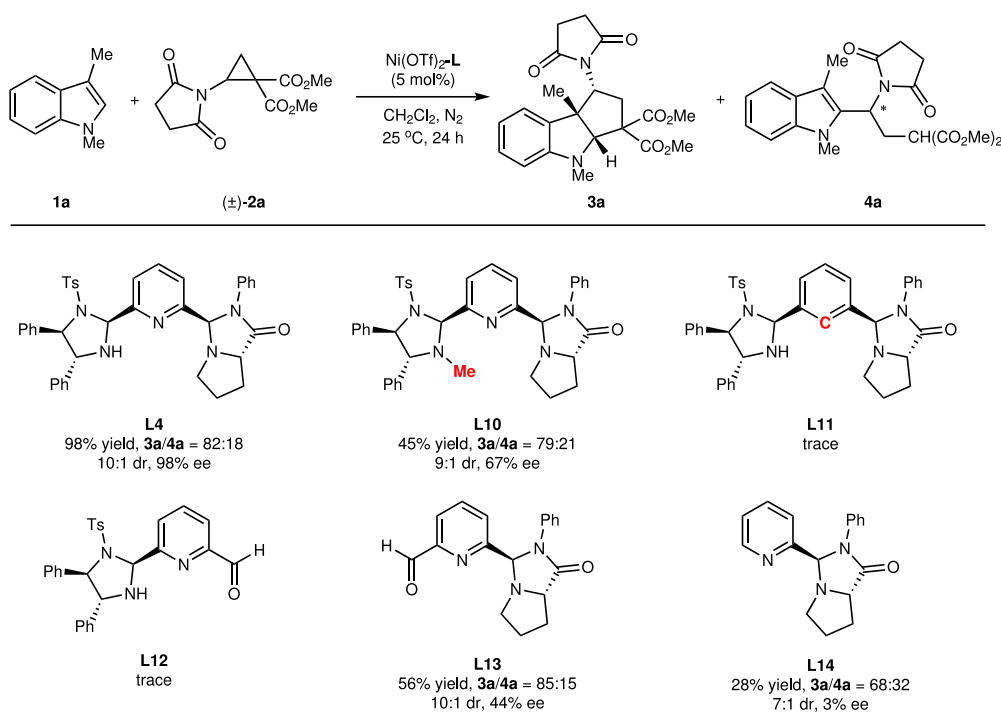


Fig. 5 | Control experiments. Reaction conditions: Ni(OTf)₂/L (1:1.2, 5 mol%), **1a** (0.1 mmol), **2a** (0.22 mmol) in CH₂Cl₂ (2.0 mL) at 25 °C under N₂ for 24 h; The total yield (**3a** + **4a**) and dr value of **3a** were determined by ¹H NMR spectra of the crude product; The ee value of **3a** was determined by chiral HPLC analysis.

The Ni(OTf)₂-PyIPI **L4**-catalyzed reaction mechanism and stereoselectivity were extensively examined by using density functional theory (DFT). Firstly, the structure of complex **c-2a** was studied in detail by theoretical calculations and X-ray crystallography, which were displayed in Supplementary Figs. 131–132. As described in Fig. 7, the mechanism consisted of a two-step process: ring-opening and ring-closing. In step 1, Ni(OTf)₂-PyIPI **L4** and (*S*)-aminocyclopropane **2a** generated complex **c-2a**, in which pentacoordinated Ni(II) formed square pyramidal geometry due to the steric repulsion of a phenyl group in the imidazolidine moiety of **L4**. PyIPI **L4** acted as a tridentate ligand with three nitrogen atoms coordinated to Ni(II) and (*S*)-**2a** as a bidentate substrate with two carbonyl oxygen atoms coordinated to Ni(II). Meanwhile, the imidazolidine NH of **L4** H-bond with the oxygen atom in succinimide moiety, and π–π stacking interaction was

observed between two aryl groups in the imidazolidine moiety. Then, the reactant complex (**RC**) was formed from indole **1a** and complex **c-2a**, followed by ring-opening of indole **1a** to (*S*)-**2a** from the indole's *Si* face via transition state **TS1** with the relative free energy of 20.7 kcal/mol. Intermediate **IM1** formed the C3-alkylation indole zwitterion.

In step 2, intermediate **IM2** was generated via bond rotation from **IM1**, which allowed restoration of H-bond between the imidazolidine NH of **L4** and the oxygen atom in succinimide moiety. The ring-closing at C2 position of the indole proceeded via transition state **TS2** with the relative free energy of 26.0 kcal/mol, affording complex **PC1**. Addition of substrate **2a** released tricyclic indoline **3a** and complex **c-2a** was regenerated. Based on the energetic span model³⁹ of catalytic cycles, the reaction rate was determined by **TS2** (26.0 kcal/mol) and **IM1** (–3.0 kcal/mol).

Furthermore, as shown in Supplementary Fig. 133, there was a bifurcating transition state⁴⁰ **TS3** between **TS1** and **IM1** in the reaction pathways. Meanwhile, the other pathway would lead to intermediate **IM3** which corresponded to product **4a**. This phenomenon corresponded to 1,2-alkyl group migration^{41–43} in the experimental study. Interestingly, from the viewpoint of the activation energy barrier, the side-pathway was energetically more favored than the main-pathway. However, from another perspective, in the dynamic competition between **IM1** and **IM3**, the nucleophilic attack of N lone pair at the nearby C2 atom in indole **1a** to form a double bond would lead to the dominant **IM1** intermediate. Importantly, the relative free energy of

IM1 was 6.4 kcal/mol lower than that of **IM3**, and was even 3.0 kcal/mol lower than reactant, which indicated that **IM1** was the high fraction stable intermediate. Thus, C3-alkylation product **3a** was the main product and was consistent with the above experiments (Table 1, entry 18).

The stereoselectivity of the [3 + 2] annulation reaction was further explored by comparing the geometry information and free energy of the enantio-determining transition states (Fig. 8). As mentioned above, the ring-closing step was the rate-determining step. The relative free energy of **TS2** was 2.4 kcal/mol ($\Delta\Delta G^\ddagger$) lower than that of *ent*-**TS2**, which suggested that (1*R*,3*aR*,8*bR*)-**3a** was the dominant adduct, and was in good agreement with the above experiments (Table 1, entry 18). The visual analysis of non-covalent interactions (NCI)⁴⁴ for *ent*-**TS2** was performed by independent gradient model based on Hirshfeld partition (IGMH)^{45,46}. As shown in the lower right corner of Fig. 8, it indicated that the observed increase of the energy barrier was mainly caused by the obvious steric repulsion between the indoline ring and phenyl group of the imidazolidine moiety. In addition, H-bond interaction between imidazolidine NH and oxygen atom in succinimide moiety in **TS2** (2.036 Å) was stronger than that of *ent*-**TS2** (2.894 Å), which was also favorable for lowering the energy barrier in Fig. 8.

Discussion

The catalytic asymmetric dearomatic [3 + 2] annulation of 3-substituted indoles with D-A aminocyclopropanes is realized. C₁-Symmetric bifunctional tridentate PyIPI ligand was rationally designed and facily synthesized with structurally tunable. With 5 mol% of Ni(OTf)₂-PyIPI **L4** complex as the catalyst, diverse tricyclic indolines were obtained in moderate to good yields, good chemoselectivities, high diastereoselectivities (up to 10:1 dr), and excellent enantioselectivities (up to 98% ee). To our surprise, PyIPI

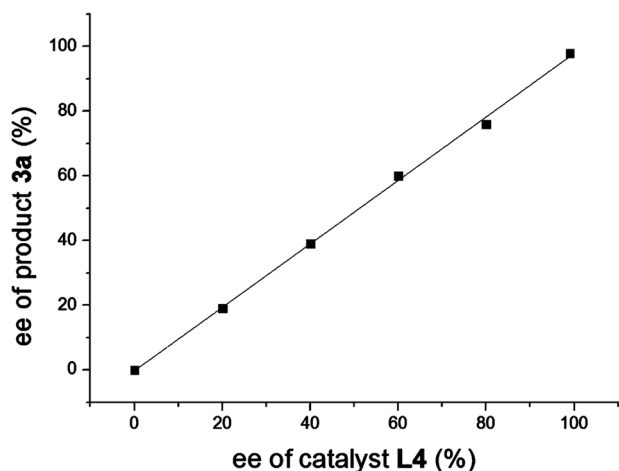


Fig. 6 | Mechanism investigation. The relationship between ee values of ligand **L4** and product **3a**.

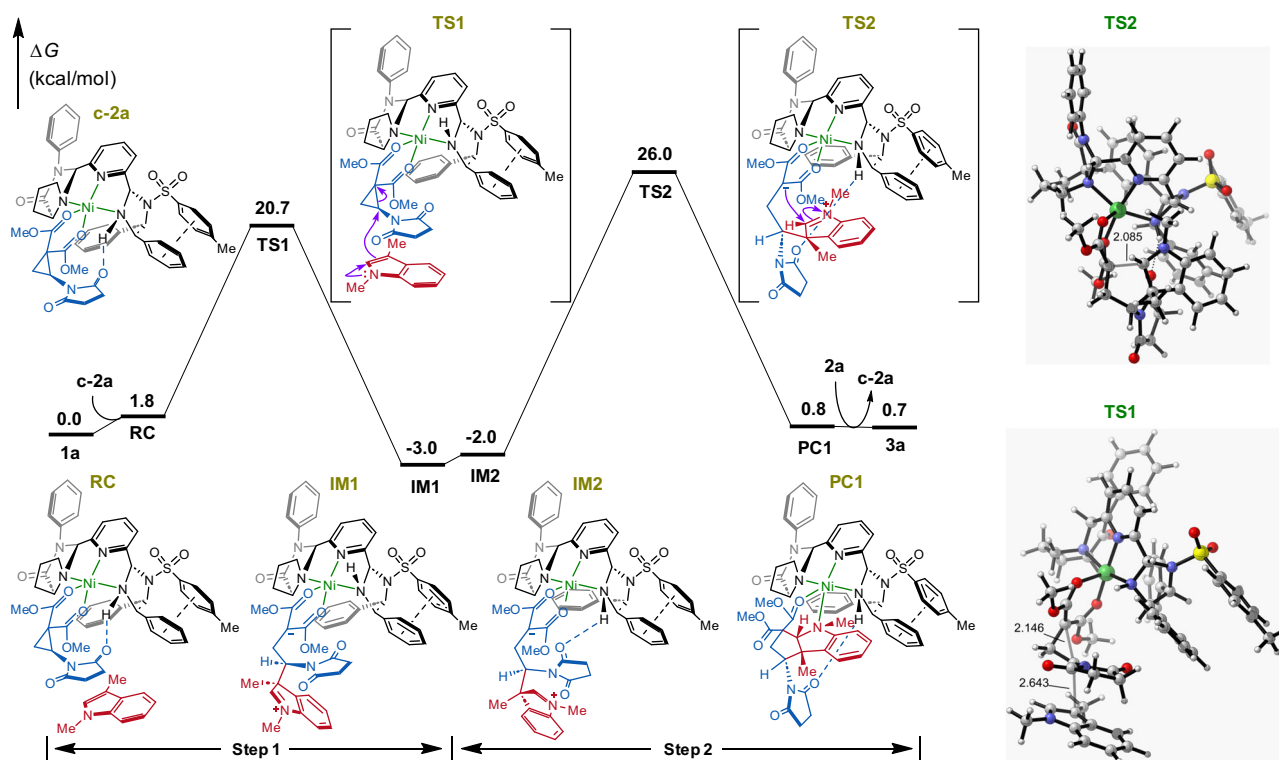


Fig. 7 | Catalytic reaction pathway. Relative energy profiles (in kcal/mol) of catalyzed reaction pathway and optimized structures of important transition state (bond lengths, Å) at the M06-2X-D3/Def2-TZVP/SMD(DCM)//M06-2X-D3/Def2-SVP level.

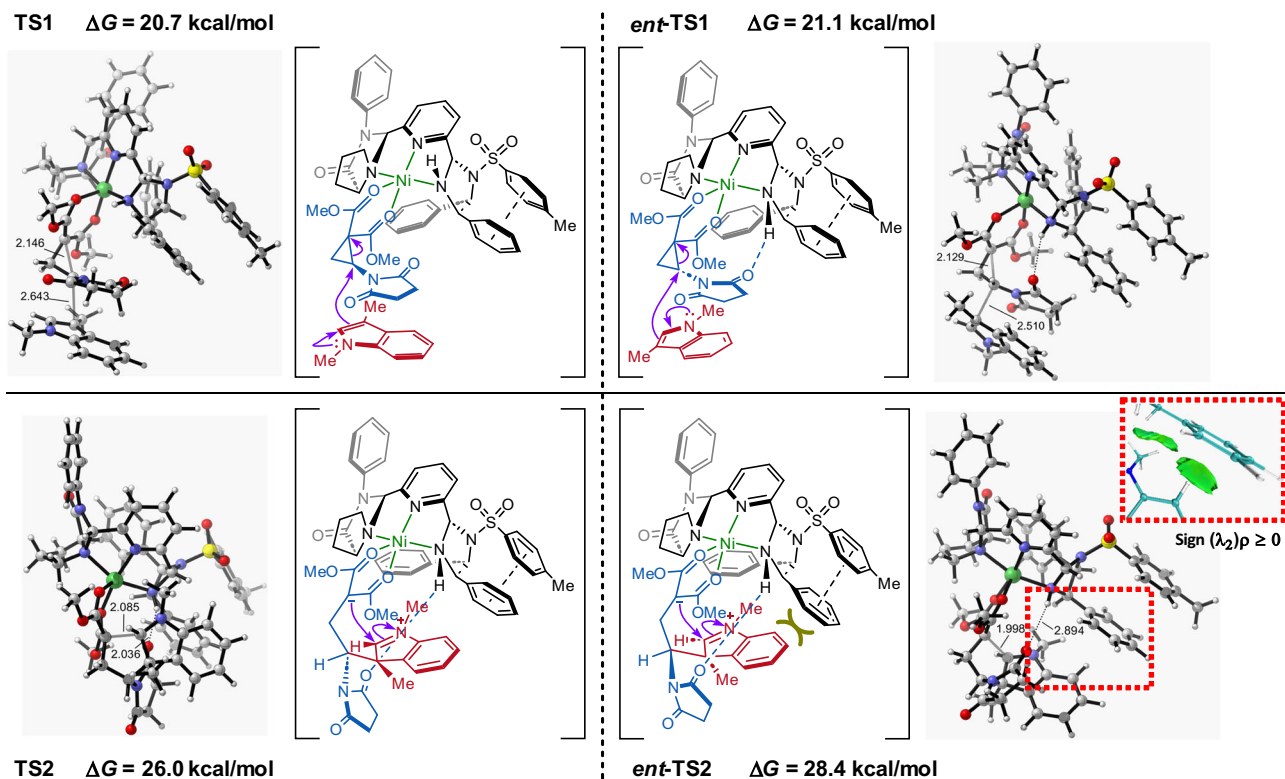


Fig. 8 | Stereocontrol mechanism. DFT-optimized structures (bond lengths, Å) and relative free energies (ΔG , kcal/mol) of enantio-determining transition states at the M06-2X-D3/Def2-TZVP/SMD(DCM)//M06-2X-D3/Def2-SVP level of theory.

L4 with an unusual *cis*-configuration was the optimal ligand, which was found to be better than C_2 -symmetric tridentate nitrogen ligands **L8** and **L9** in the annulation reaction. A series of control experiments, as well as single crystal structure of PyIPI **L1**-Cu(OTf)₂ complex, linear correlation experiment, and DFT calculations, revealed a dual activation mechanism, where the tridentate nitrogen atoms coordinated with Ni(II) to activate aminocyclopropane via bidentate coordination with the geminal diester, followed by imidazolidine NH formed a H-bond with the oxygen atom in succinimide moiety. In addition, high enantioselectivity of the reaction was governed by steric factors. Further applications of chiral PyIPI in other metal-catalyzed asymmetric reactions are currently underway in our research group.

Methods

Typical procedure for the synthesis of PyIPI ligand

Pyridine-2,6-dicarbaldehyde (20.0 mmol) and *L*-prolinamides (10.0 mmol) were added to a pressure-resistant test tube with anhydrous ethanol (30.0 mL). Then, the reaction was heated and stirred at 60 °C for 3 h. After that, the reaction mixture was concentrated in vacuo to remove ethanol. The residue was purified by flash column chromatography (Pet/EtOAc, 10/1-1/1, v/v) to give the one-sided condensation product. Then, in a round-bottomed flask containing a stir bar, the above one-sided condensation product (1.0 mmol), (*R,R*)-diphenylethylenediamine (1.0 mmol), CH₃CO₂H (1.5 mmol, 74.0 μ L), and dichloromethane (6.0 mL) were added. Then, the reaction was stirred at 30 °C under N₂ for 6–8 h. After that, the reaction mixture was quenched by aqueous NaHCO₃. The organic layer was extracted with dichloromethane for 3 times, and the collected organic layer was dried over Na₂SO₄. After removing the solvent under reduced pressure, the resulting residue was purified by silica gel column chromatography to give the corresponding PyIPI ligand.

Typical procedure for the catalytic asymmetric dearomative [3 + 2] annulation

In a dry reaction tube, a mixture of Ni(OTf)₂ (3.6 mg, 0.01 mmol, 5 mol%), ligand **L4** (7.9 mg, 0.012 mmol, 6 mol%), and aminocyclopropane **2** (0.44 mmol) in DCM (3.0 mL) were stirred at room temperature for 30 minutes under the atmosphere of nitrogen. Then indole substrate **1** (0.2 mmol) in DCM (1.0 mL) was added to the mixture of catalyst via a syringe. After 24 h, the reaction was complete (monitored by TLC). The reaction was filtered through a glass funnel within layer of silica gel (100–200 mesh) and purified by flash column chromatography (Pet/EtOAc, v/v, 10:1-2:1) to give the product **3**.

Data availability

The data that support the findings of this study is available within the main text and its Supplementary Information file. Source data is provided as Source data file. Data is also available from the corresponding author upon request. The X-ray crystallographic coordinates for structures reported in this study have been deposited at the Cambridge Crystallographic Data Centre (CCDC), under deposition numbers 2203570 (**L1**-Cu(OTf)₂ complex), 2203566 (**L3**), 2203567 (**L4**), 2203568 (**L8**), 2203569 (**L13**), 2203571 (**3a**), and 2203572 (\pm **3o'**). These data can be obtained free of charge from The Cambridge Crystallographic Data Centre via www.ccdc.cam.ac.uk/data_request/cif.

References

- Zhang, G., Catalano, V. J. & Zhang, L. PtCl₂-catalyzed rapid access to tetracyclic 2,3-indoline-fused cyclopentenes: reactivity divergent from cationic Au(I) catalysis and synthetic potential. *J. Am. Chem. Soc.* **129**, 11358–11359 (2007).
- Qin, B., Lu, Z. & Jia, Y. Divergent total synthesis of four kopsane alkaloids: *N*-carbomethoxy-10,22-dioxokopsane, epikopsanol-10-lactam, 10,22-dioxokopsane, and *N*-methylkopsanone. *Angew. Chem. Int. Ed.* **61**, e202201712 (2022).

3. Bin, H.-Y. et al. Scalable enantioselective total synthesis of (-)-goniomitine. *Angew. Chem. Int. Ed.* **58**, 1174–1177 (2019).
4. Zhuo, C.-X., Zhang, W. & You, S.-L. Catalytic asymmetric dearomatization reactions. *Angew. Chem. Int. Ed.* **51**, 12662–12686 (2012).
5. Zhuo, C.-X., Zheng, C. & You, S.-L. Transition-metal-catalyzed asymmetric allylic dearomatization reactions. *Acc. Chem. Res.* **47**, 2558–2573 (2014).
6. Roche, S. P., Tendoung, J.-J. Y. & Tréguier, B. Advances in dearomatization strategies of indoles. *Tetrahedron* **71**, 3549–3591 (2015).
7. Zheng, C. & You, S.-L. Catalytic asymmetric dearomatization by transition-metal catalysis: a method for transformations of aromatic compounds. *Chem* **1**, 830–857 (2016).
8. Zheng, C. & You, S.-L. Catalytic asymmetric dearomatization (CADA) reaction-enabled total synthesis of indole-based natural products. *Nat. Prod. Rep.* **36**, 1589–1605 (2019).
9. Sheng, F.-T., Wang, J.-Y., Tan, W., Zhang, Y.-C. & Shi, F. Progresses in organocatalytic asymmetric dearomatization reactions of indole derivatives. *Org. Chem. Front.* **7**, 3967–3998 (2020).
10. Zheng, C. & You, S.-L. Advances in catalytic asymmetric dearomatization. *ACS Cent. Sci.* **7**, 432–444 (2021).
11. Liang, R.-X. & Jia, Y.-X. Aromatic π -components for enantioselective Heck reactions and Heck/anion-capture domino sequences. *Acc. Chem. Res.* **55**, 734–745 (2022).
12. Xiong, H., Xu, H., Liao, S., Xie, Z. & Tang, Y. Copper-catalyzed highly enantioselective cyclopentannulation of indoles with donor–acceptor cyclopropanes. *J. Am. Chem. Soc.* **135**, 7851–7854 (2013).
13. Zhu, J. et al. Remote ester groups switch selectivity: diastereodivergent synthesis of tetracyclic spiroindolines. *J. Am. Chem. Soc.* **136**, 6900–6903 (2014).
14. Liao, S., Sun, X.-L. & Tang, Y. Side arm strategy for catalyst design: modifying bisoxazolines for remote control of enantioselection and related. *Acc. Chem. Res.* **47**, 2260–2272 (2014).
15. Liu, Q.-J., Yan, W.-G., Wang, L., Zhang, X. P. & Tang, Y. One-pot catalytic asymmetric synthesis of tetrahydrocarbazoles. *Org. Lett.* **17**, 4014–4017 (2015).
16. Yan, W.-G., Wang, P., Wang, L., Sun, X.-L. & Tang, Y. Copper catalyzed [3+2] annulation of indoles with 1,1,2,2-tetrasubstituted donor-acceptor cyclopropanes. *Acta Chim. Sin.* **75**, 783–787 (2017).
17. Zhou, L., Yan, W.-G., Sun, X.-L., Wang, L. & Tang, Y. A versatile enantioselective catalytic cyclopropanation-rearrangement approach to the divergent construction of chiral spiroaminals and fused bicyclic acetals. *Angew. Chem. Int. Ed.* **59**, 18964–18969 (2020).
18. De Nanteuil, F., Loup, J. & Waser, J. Catalytic Friedel-Crafts reaction of aminocyclopropanes. *Org. Lett.* **15**, 3738–3741 (2013).
19. Liu, H.-K. et al. Selectivity switch in a rhodium(II) carbene triggered cyclopentannulation: divergent access to three polycyclic indolines. *Angew. Chem. Int. Ed.* **58**, 4345–4349 (2019).
20. Pirenne, V., Robert, E. G. L. & Waser, J. Catalytic (3+2) annulation of donor-acceptor aminocyclopropane monoesters and indoles. *Chem. Sci.* **12**, 8706–8712 (2021).
21. Nishiyama, H. et al. Chiral and C₂-symmetrical bis(oxazoliny)pyridine/rhodium(III) complexes: effective catalysts for asymmetric hydrosilylation of ketones. *Organometallics* **8**, 846–848 (1989).
22. Owens, T. D., Hollander, F. J., Oliver, A. G. & Ellman, J. A. Synthesis, utility, and structure of novel bis(sulfinyl)imidamidate ligands for asymmetric Lewis acid catalysis. *J. Am. Chem. Soc.* **123**, 1539–1540 (2001).
23. Yoon, T. P. & Jacobsen, E. N. Privileged chiral catalysts. *Science* **299**, 1691–1693 (2003).
24. Desimoni, G., Faita, G. & Quadrelli, P. Pyridine-2,6-bis(oxazolines), helpful ligands for asymmetric catalysts. *Chem. Rev.* **103**, 3119–3154 (2003).
25. Bhor, S. et al. Synthesis of a new chiral N,N,N-tridentate pyridinebisimidazoline ligand library and its application in Ru-catalyzed asymmetric epoxidation. *Org. Lett.* **7**, 3393–3396 (2005).
26. Langlotz, B. K., Wadepohl, H. & Gade, L. H. Chiral bis(pyridylimino)isoindoles: a highly modular class of pincer ligands for enantioselective catalysis. *Angew. Chem. Int. Ed.* **47**, 4670–4674 (2008).
27. Li, C. et al. Asymmetric ruthenium-catalyzed hydrogenation of terpyridine-type N-heteroarenes: direct access to chiral tridentate nitrogen ligands. *Org. Lett.* **22**, 6452–6457 (2020).
28. Wang, H., Wen, J. & Zhang, X. Chiral tridentate ligands in transition metal-catalyzed asymmetric hydrogenation. *Chem. Rev.* **121**, 7530–7567 (2021).
29. Ye, W. et al. Highly active ruthenium(II) complex catalysts bearing an unsymmetrical NNN ligand in the (asymmetric) transfer hydrogenation of ketones. *Chem. Eur. J.* **17**, 4737–4741 (2011).
30. Monfette, S., Turner, Z. R., Semproni, S. P. & Chirik, P. J. Enantiopure C₁-symmetric bis(imino)pyridine cobalt complexes for asymmetric alkene hydrogenation. *J. Am. Chem. Soc.* **134**, 4561–4564 (2012).
31. Zhang, L., Zuo, Z., Wan, X. & Huang, Z. Cobalt-catalyzed enantioselective hydroboration of 1,1-disubstituted aryl alkenes. *J. Am. Chem. Soc.* **136**, 15501–15504 (2014).
32. Chen, J., Xi, T. & Lu, Z. Iminopyridine oxazoline iron catalyst for asymmetric hydroboration of 1,1-disubstituted aryl alkenes. *Org. Lett.* **16**, 6452–6455 (2014).
33. Guo, J., Cheng, Z., Chen, J., Chen, X. & Lu, Z. Iron- and cobalt-catalyzed asymmetric hydrofunctionalization of alkenes and alkynes. *Acc. Chem. Res.* **54**, 2701–2716 (2021).
34. Arai, T., Mishiro, A., Yokoyama, N., Suzuki, K. & Sato, H. Chiral bis(imidazolidine)pyridine–Cu(OTf)₂: catalytic asymmetric endo-selective [3+2] cycloaddition of imino esters with nitroalkenes. *J. Am. Chem. Soc.* **132**, 5338–5339 (2010).
35. Arai, T. et al. PyBidine–Cu(OTf)₂-catalyzed asymmetric [3+2] cycloaddition with imino esters: harmony of Cu–Lewis Acid and imidazolidine-NH hydrogen bonding in concerted catalysis. *Angew. Chem. Int. Ed.* **54**, 1595–1599 (2015).
36. Uozumi, Y., Mizutani, K. & Nagai, S.-I. A parallel preparation of a bicyclic N-chiral amine library and its use for chiral catalyst screening. *Tetrahedron Lett.* **42**, 407–410 (2001).
37. Uozumi, Y. & Shibatomi, K. Catalytic asymmetric allylic alkylation in water with a recyclable amphiphilic resin-supported P,N-chelating palladium complex. *J. Am. Chem. Soc.* **123**, 2919–2920 (2001).
38. Wang, X.-B. et al. Rational design of chiral tridentate ligands: bifunctional cobalt(II) complex/hydrogen bond for enantioselective Michael reactions. *Org. Lett.* **24**, 3861–3866 (2022).
39. Kozuch, S. & Shaik, S. How to conceptualize catalytic cycles? the energetic span model. *Acc. Chem. Res.* **44**, 101–110 (2011).
40. Yang, Z. et al. Relationships between product ratios in ambimodal pericyclic reactions and bond lengths in transition structures. *J. Am. Chem. Soc.* **140**, 3061–3067 (2018).
41. Kerr, M. A. & Keddy, R. G. The annulation of 3-alkylindoles with 1,1-cyclopropane diesters. *Tetrahedron Lett.* **40**, 5671–5675 (1999).
42. England, D. B., Kuss, T. D. O., Keddy, R. G. & Kerr, M. A. Cyclopentannulation of 3-alkylindoles: a synthesis of a tetracyclic subunit of the kopsane alkaloids. *J. Org. Chem.* **66**, 4704–4709 (2001).
43. England, D. B., Woo, T. K. & Kerr, M. A. The reactions of 3-alkylindoles with cyclopropanes: an unusual rearrangement leading to 2,3-disubstitution. *Can. J. Chem.* **80**, 992–998 (2002).
44. Johnson, E. R. et al. Revealing noncovalent interactions. *J. Am. Chem. Soc.* **132**, 6498–6506 (2010).
45. Lu, T. & Chen, F. Multiwfn: a multifunctional wavefunction analyzer. *J. Comput. Chem.* **33**, 580–592 (2012).
46. Lu, T. & Chen, Q. Independent gradient model based on Hirshfeld partition: a new method for visual study of interactions in chemical systems. *J. Comput. Chem.* **43**, 539–555 (2022).

Acknowledgements

We are grateful for the financial support from NSFC (Nos. 21971056, M.-S.X.; 22071046, H.-M.G.; and U22A20378, H.-M.G.), Zhongyuan Scholar (212101510004, H.-M.G.), and the Natural Science Foundation of Henan Province (202300410224, M.-S.X.; and 222300420474, H.-X.W.), the Key Project for Science and Technology Research of Henan Provincial Department (21A150001, H.-X.W.), and Program for Innovative Research Team in Science and Technology in University of Henan Province (23IRTSTHN003, M.-S.X.; and 22IRTSTHN003, M.-S.X.). We also thank the financial support from Henan Key Laboratory of Organic Functional Molecules and Drug Innovation, and NMPA Key Laboratory for Research and Evaluation of Innovative Drug.

Author contributions

M.-S.X. and H.-M.G. designed the ligands. H.-X.W. and C.Y. synthesized the ligands. H.-X.W., C.Y., and B.-Y.X. performed the experiments. Y.T. and C.P. performed the computational studies. M.-S.X. and H.-M.G. supervised the work. M.-S.X. and Y.T. co-wrote the original draft. M.-S.X., Y.T., and H.-M.G. co-wrote the final manuscript.

Competing interests

The authors declare no competing interests.

Additional information

Supplementary information The online version contains supplementary material available at <https://doi.org/10.1038/s41467-023-38059-7>.

Correspondence and requests for materials should be addressed to Ming-Sheng Xie, Yin Tian or Hai-Ming Guo.

Peer review information *Nature Communications* thanks the anonymous reviewers for their contribution to the peer review of this work.

Reprints and permissions information is available at <http://www.nature.com/reprints>

Publisher's note Springer Nature remains neutral with regard to jurisdictional claims in published maps and institutional affiliations.

Open Access This article is licensed under a Creative Commons Attribution 4.0 International License, which permits use, sharing, adaptation, distribution and reproduction in any medium or format, as long as you give appropriate credit to the original author(s) and the source, provide a link to the Creative Commons license, and indicate if changes were made. The images or other third party material in this article are included in the article's Creative Commons license, unless indicated otherwise in a credit line to the material. If material is not included in the article's Creative Commons license and your intended use is not permitted by statutory regulation or exceeds the permitted use, you will need to obtain permission directly from the copyright holder. To view a copy of this license, visit <http://creativecommons.org/licenses/by/4.0/>.

© The Author(s) 2023